

Green hydrogen production pathways: Comparative insights from Denmark, the United States, and China

Elisabeth Andreae^a, Yuanbei F. Fan^b, Marianne Petersen^{a,c}, Shi You^a, Henrik W. Bindner^a, Mark Z. Jacobson^b

^a Technical University of Denmark (DTU), Department of Wind and Energy Systems, Frederiksborgvej 399, Roskilde, 4000, Denmark

^b Stanford University, Department of Civil and Environmental Engineering, 473 Via Ortega, Stanford, 94305, United States of America

^c Siemens Gamesa Renewable Energy, Borupvej 16, Brande, 7330, Denmark

ARTICLE INFO

Keywords:

Power-to-X
System design
Hydrogen
Operation principle
Case based analysis

ABSTRACT

In the pursuit of reducing carbon emissions in hard-to-decarbonize sectors such as heavy industry and shipping, power-to-hydrogen technology offers a promising pathway. The technology uses water electrolysis to convert renewable energy into hydrogen, which can then be used directly as hydrogen fuel with a fuel cell to produce electricity for transportation or grid balancing or used for steel, ammonia, and methanol production. This study evaluates and compares power-to-hydrogen systems by examining system scale, geographical conditions, design choices, configuration, operational strategies, and other key factors critical in shaping system performance. Efficiency and cost are assessed as separate but related aspects influencing the overall viability of green electrolyzer systems (electrolyzers powered by clean, renewable electricity). The analysis of power-to-hydrogen systems in Denmark, the United States, and China reveals variations in costs, technological approaches, and strategic implementations across these regions. The comparative evaluation shows that the economic viability of these systems is largely driven by design choices and operational strategies. The findings highlight that customizing power-to-hydrogen systems to local conditions is essential for achieving optimal cost-effectiveness.

1. Introduction

Power-to-X (PtX) is emerging as a pivotal technology enabling the global energy transition. PtX refers to the conversion of surplus renewable electricity into alternative fuels such as green hydrogen (H₂) and its derivatives, which can be utilized across various sectors, like transportation, heavy industry, and agriculture [1]. As countries intensify efforts to reach net-zero emissions, green H₂ has become a critical bridge between renewable energy generation and hard-to-abate sectors, offering a versatile solution for large-scale energy storage, sector coupling, and global energy trade. Among PtX technologies, those that produce hydrogen are commonly referred to as power-to-hydrogen (PtH) technologies.

The techno-economic feasibility of green H₂ production varies depending on regional factors, such as renewable resource availability, electricity market structures, infrastructure maturity, and policy frameworks. A country-level comparison is essential to understand how national contexts shape the cost-effective and scalable H₂ deployment strategies.

A growing body of research focuses on integrating renewable energy sources, employing probabilistic modeling methods, and incorporating

geographically specific factors in the techno-economic analysis and system optimization of H₂ production technologies.

Several recent studies have expanded methods for analyzing H₂ production systems across diverse contexts. For instance, Baral et al. (2024) evaluated eight hybrid renewable systems for green H₂ production, including scenarios with Organic Rankine Cycle (ORC) integration to enhance waste heat recovery [2]. Similarly, Wolf et al. (2024) used Monte Carlo simulations to estimate the Levelized Cost of Hydrogen (LCoH) for multiple countries, highlighting regional competitiveness for future H₂ exports to Germany [3].

In a microgrid application, Urs et al. (2023) modeled a green H₂-based energy system for a commercial building in the UAE, demonstrating economic viability under current and projected utility rates [4]. Meanwhile, Luo et al. (2020) presented a detailed cost model for H₂ production in China's transport sector, emphasizing the cost drivers associated with renewable versus fossil fuel-based production pathways [5].

Advanced modeling approaches are also increasingly adopted. Superchi et al. (2023) conducted a large-scale parametric simulation

* Corresponding author.

E-mail address: elisan@dtu.dk (E. Andreae).

(84,240 scenarios) for wind-powered green H₂ production in Italy's steelmaking sector, demonstrating that decarbonization goals can be economically feasible under optimized system configurations [6]. Zheng et al. (2023) applied operational and market optimization models to assess the profitability of PtH systems providing grid services in Denmark [7] and designed detailed wind-to-H₂ systems with high-resolution wind modeling for off-grid scenarios [8].

On a global scale, Makepeace et al. (2024) developed a comprehensive techno-economic model for evaluating green H₂ export supply chains, integrating production, transport, and re-conversion costs with stochastic uncertainty analyses [9]. Jacobson et al. (2023) show that integrating green H₂ into steel, ammonia, and transport sectors within 100% wind, water, and solar systems can be achieved without substantially increasing overall electricity costs, reinforcing H₂'s viability in deep decarbonization strategies [10]. Building on this, Jacobson et al. (2024) demonstrate how H₂ complements batteries in grid storage solutions to ensure cost-effective and reliable electricity supply, with the optimal mix depending on regional demand profiles and storage needs [11].

The reviewed literature reveals several common themes and innovative approaches in research methods for assessing the techno-economic feasibility of H₂ production. All studies emphasize the importance of economic analyses that incorporate both capital and operational expenditures. Sensitivity analyses are frequently employed to understand the impact of various cost factors, such as raw material prices and carbon trading costs. The integration of renewable electricity sources, like solar and wind, is a recurring theme, with many studies highlighting the benefits of using electrolysis for H₂ production. The studies consistently underscore three key themes:

- Integration of renewables: Solar PV, onshore and offshore wind, often hybridized with storage solutions, remain the dominant energy sources.
- Probabilistic and operational modeling: Increasing use of Monte Carlo simulations, mixed-integer programming, and high-resolution datasets to better capture uncertainties and operational constraints.
- Focus on cost reduction: Through design optimization, scale-up, and improved electrolyzer technologies, many studies identify pathways to lower H₂ costs to below 2 \$/kg by 2030 in favorable locations.

Recent research continues to emphasize renewable integration, system efficiency, and cost competitiveness in the techno-economic optimization of H₂ production systems. Studies show that while gray H₂ remains the cheapest option today, policy incentives and carbon pricing are rapidly shifting investment viability toward blue and green H₂, particularly in regions with abundant renewable resources [12]. Optimization frameworks now consider not only production efficiency but also the storage challenges associated with H₂'s low volumetric energy density, which imposes substantial cost and energy penalties for compression and liquefaction [13]. Innovations such as waste heat recovery through ORC systems in multi-megawatt electrolyzers have further improved overall process efficiencies by up to 25%, although their economic viability remains highly sensitive to local electricity prices [14]. Together, these developments reflect a maturing research field that increasingly addresses both technical and market uncertainties.

Nevertheless, important gaps persist. While many studies model national or regional systems, there is still limited analysis that dynamically integrates cross-border H₂ trade under realistic policy and financial risk scenarios. Furthermore, although techno-economic studies increasingly incorporate operational uncertainties, comprehensive lifecycle emissions assessments beyond basic carbon accounting remain sparse.

Another critical limitation is that most techno-economic analyses focus on isolated national cases, idealized system designs, or theoretical optimization under perfect market conditions. The existing

literature lacks comparative studies that systematically incorporate regional variations in capacity pricing, renewables availability, system configurations, and scaling effects on cost and performance outcomes. This gap is particularly important, as regional disparities in renewable energy profiles, infrastructure readiness, and economic structures can substantially alter the feasibility and cost trajectories of PtH systems. Without regionally grounded insights, strategies for large-scale green H₂ deployment risk being either overgeneralized or poorly adapted to specific national contexts.

In light of these gaps, the present study hypothesizes that:

Regional differences in renewable resource profiles and infrastructure maturity shape the cost-effectiveness and operational performance of PtH systems, and that tailored system configurations can improve economic feasibility in each national context.

To test this hypothesis, a comparative method is developed that systematically accounts for regional factors, system design choices, and scaling effects across Denmark, China, and the United States (U.S.). The study analyzes how variations in production scale, geographical conditions, configurations, and operational strategies influence key performance metrics such as electricity output and cost-effectiveness.

A techno-economic assessment is conducted to understand how the cost structure of the PtH systems differs based on system types, configurations, and operational scenarios. The analysis identifies key cost drivers and evaluates how scaling impacts electrolyzer investment costs, providing insights into potential cost reductions as system size increases. The study further examines the influence of technical and economic factors on the feasibility and operational performance of PtH systems across different regions, providing a comparative evaluation of their strategic role in achieving carbon neutrality.

Notably, the analysis reveals a very large cost difference between the Chinese system and the other systems assessed. This reflects structural differences in cost levels, market conditions, and financing environments that affect the comparability of the results. While the analysis provides useful insights into relative cost structures and system dynamics, these disparities should be considered when interpreting the results, as they may influence the perceived competitiveness across regions. This limitation is further addressed in the discussion, particularly in Section 3.3, where qualitative trends and systemic implications are emphasized over absolute cost comparisons.

The article is organized as follows: Section 2 outlines the method used to compare three different PtH systems across various locations. Section 3 presents the results of this comparison, focusing on system operation, sizing, and costs. Section 4 offers a discussion of the findings, and Section 5 concludes the study.

2. Methods

This section outlines the methods used to optimize the design of PtH systems with the objective of minimizing the Levelized Cost of Energy (LCoE). A PtH system typically includes several components, with the electrolyzer serving as the central unit for H₂ production. For green H₂ production, the electricity supplied to the system must come from renewable sources. The optimization focuses on determining the optimal sizing of key system units – specifically the electrolyzer and associated energy storage – while the capacities of the renewable generation units are held constant. Both capital expenditures (CAPEX) and operational expenditures (OPEX) are incorporated into the economic evaluation to capture the full lifecycle costs.

A central methodological feature involves CAPEX scaling for electrolyzers to reflect non-linear cost reductions with increasing system size. Empirical scaling factors are applied to capture the non-linear cost behavior of electrolyzer systems, visible for electrolyzer capacities below 100 MW. Accurate scaling of capital costs ensures realistic estimation of investment requirements across different system configurations.

The optimization process employs a modified version of the Hooke–Jeeves direct search algorithm to identify system designs that minimize the LCoE under specified operating conditions. The analysis is applied to compare three national cases: Denmark, China, and the U.S. An overview of the system units, cost modeling, and optimization approach is provided in the following subsections.

2.1. The Hooke–Jeeves algorithm for optimization

The Hooke–Jeeves algorithm is a direct optimization method for finding the minimum of an objective function [15]. The method explores the design space by taking small steps in each coordinate direction to evaluate its respective objective value. At every iteration, it starts at an anchoring design point x_0 where it assesses its objective value $f(x_0)$ and evaluates $f(x + \alpha e^i)$ for a given step size α for each unique coordinate direction i . The method accepts any improvements it discovers, and if no improvements are found in the current iteration, it reduces the step size and repeats the search. The search process stops and returns an “optimal” value when the step size is smaller than a defined tolerance value.

For an n -dimensional problem, each iteration of the Hooke–Jeeves method requires $2n$ function evaluations, which can be computationally expensive for problems with a large dimensionality. The method is prone to getting stuck in local minima, although it has been proven to converge for certain classes of functions.

2.1.1. Levelized cost of energy as the objective function

The economic performance assessment is carried out by calculating the LCoE. This metric reflects the average production cost per unit of energy over the system’s entire lifespan, including both direct expenses and capital expenditures required for project implementation. The LCoE calculation follows the method outlined in [16], with LCoE defined as shown in Eq. (1).

$$LCoE = \frac{CAPEX + \sum_{t=1}^N \frac{OPEX_t^{fix} + OPEX_t^{var} + F_t}{(1+r)^t}}{\sum_{t=1}^N \frac{E_t}{(1+r)^t}} \quad (1)$$

The CAPEX represents the initial investment. The $OPEX_t^{fix}$ and $OPEX_t^{var}$, refer to the annual fixed and variable operations and maintenance costs, respectively. F_t indicates the fuel cost in year t , N signifies the expected system or asset lifetime, and r denotes the applied discount rate. All costs are expressed in USD (2024), with currency conversions based on rates from [17], consistent with the values shown in Table 3. Because the systems studied in the three cases produce different final outputs (H_2 in some cases and electricity in others) a consistent comparison requires evaluating all systems based on the economic value of the energy they generate, regardless of its form. E_t represents the energy content of the final product of the system in year t , whether it is electricity or H_2 . For all three systems, the LCoE is evaluated to be a comparable metric.

Using a rule-based model and given operating conditions, the Hooke–Jeeves algorithm is employed to minimize the LCoE of the three systems. While renewable generation capacities are fixed, the algorithm identifies the optimal capacities for the electrolyzer and energy storage options to minimize LCoE which includes the capacity cost, operation cost, and a Value of Lost Load (VoLL). The VoLL represents the economic impact of electricity not delivered during supply disruptions [18].

Eq. (2) shows the updated LCoE function with the VoLL cost V_t of unmet demand, and with fuel cost and variable OPEX removed.

$$LCoE = \frac{CAPEX + \sum_{t=1}^N \frac{OPEX_t^{fix} + V_t}{(1+r)^t}}{\sum_{t=1}^N \frac{E_t}{(1+r)^t}} \quad (2)$$

The algorithm begins by setting an initial design point, x_0 , which defines the capacities of the electrolyzer and energy storage units, and

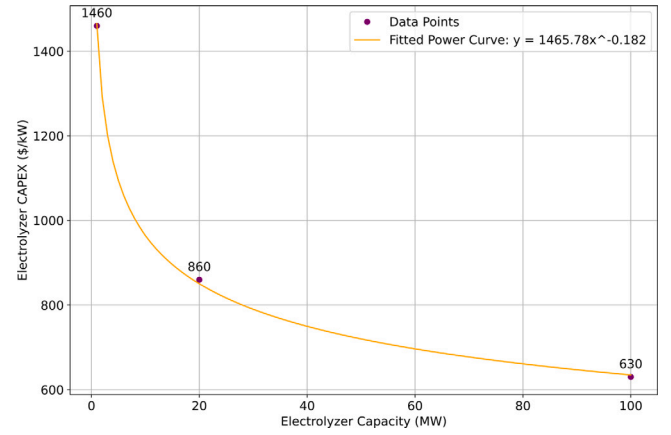


Fig. 1. Electrolyzer CAPEX scaling function derived from Lazard [19].

evaluates the corresponding objective value, $f(x_0)$, representing the system’s LCoE.

This study applies a modification to the Hooke–Jeeves algorithm by using a variable-specific proportional step size adjustment. Rather than using a fixed absolute step size α for all variables, step sizes are scaled relative to the magnitude of each variable. Specifically, the step size in each direction is given by $\zeta \cdot x_k$, where x_k is the current value of the variable in dimension k , and ζ is the step ratio. This modification addresses the challenge of dimension mismatch between variables, as e.g. the H_2 tank capacity might have a value on the order of 10^5 , while the electrolyzer capacity may be on the order of 10^3 . By ensuring the step size remains meaningful relative to each variable’s magnitude, the search space remains balanced, avoiding steps that are disproportionately large or small depending on the variable.

This proportional approach serves a similar purpose to formal normalization methods, which rescale all variables to a common, dimensionless range (e.g., 0–1). However, given the static nature and defined units of the design variables in this study, the proportional step adjustment was deemed sufficient and more transparent, maintaining the interpretability of results within the variable’s actual units. Future research may explore the use of normalization techniques, particularly when extending the model to more complex, multi-dimensional, or dynamic optimization scenarios.

2.1.2. Scaling of the capital cost of electrolyzers

When assessing the CAPEX for electrolyzers of different sizes, it is vital to account for scaling factors that represent non-linear cost variations. The baseline CAPEX offers the initial cost estimate for a specific-sized electrolyzer, but as the size changes, costs do not follow a linear trend. To provide precise CAPEX estimates for varying electrolyzer sizes, this study uses scaling factors derived from Lazard’s annual LCoH report [19], which demonstrates an exponential relationship between the size of the electrolyzer stack and the CAPEX in \$/kW, as illustrated in Fig. 1.

It is important to note that the scaling effect is most visible when the electrolyzer capacity is below 20 MW. As the capacity approaches 100 MW, the effect diminishes, and beyond this point, the cost per capacity unit does not decrease as much because the scaling function flattens.

By applying this relationship, the CAPEX for different-sized electrolyzers is calculated. These values are then normalized by dividing by the baseline CAPEX (of a 10 MW electrolyzer) to determine the scaling factors.

These scaling factors are then used to accurately adjust the CAPEX values in this study.

While the main application of the developed method is to compare PtH systems across Denmark, China, and the U.S., the analytical

framework itself is general and flexible. The approach can be applied to a wide range of PtH system designs, geographic contexts, and technological configurations. The method relies on modular modeling of system components (electrolyzer, energy storage, renewable input) and incorporates location-specific parameters such as renewable energy availability, technology costs, and discount rates. This structure enables adaptation to different regions, energy systems, or future technology scenarios without fundamentally altering the model.

Moreover, by optimizing system design based on minimizing LCoE while accounting for non-linear cost scaling and operational penalties (such as VoLL for unmet demand), the framework supports not only techno-economic comparisons but also system planning and investment analysis. It is particularly suited for early-stage feasibility assessments, sensitivity studies across different cost and performance assumptions, and scenario analyses involving future cost reductions or changing renewable energy profiles. Thus, the method developed here can inform decision-making for PtH deployment strategies in diverse regional, national, or even microgrid contexts.

2.2. Case studies

Denmark, China, and the U.S. are among the nations actively pursuing PtH strategies to meet their ambitious climate goals. Denmark is in the early stages of PtH development, aiming to establish 4–6 GW of electrolyzer capacity by 2030, supported by a DKK 1.25 billion (USD 186 million) tender in 2023 [20], adding to over DKK 3 billion (USD 432 million) invested since 2019 [21]. Denmark seeks to become a net exporter of green energy, while also improving grid efficiency and utilizing surplus heat from H₂ production [22].

In the U.S., the Department of Energy's (U.S. DOE) National Clean Hydrogen Strategy and Roadmap outlines a plan for large-scale H₂ production by 2030, backed by \$9.5 billion from the 2021 Bipartisan Infrastructure Law and tax credits from the 2022 Inflation Reduction Act. This strategy focuses on establishing Regional Clean Hydrogen Hubs and advancing electrolysis and fuel cell technology to enhance global competitiveness [23].

Meanwhile, China is aggressively investing in H₂ infrastructure, aiming to produce 100,000 to 200,000 tonnes of green H₂ annually by 2025 and expanding to 3.5 million tonnes by 2030. With over 400 H₂ refueling stations, the largest network globally, China supports its growth through initiatives like the Renewable Hydrogen 100 Action Initiative, targeting 100 GW of electrolyzer capacity by 2030. China's centralized approach, large-scale projects like Sinopec (a \$2.9 billion investment [24]) in Xinjiang, and global partnerships position it as a key player in the transition to a sustainable energy future [25].

Green H₂ production costs differ between Denmark, the U.S. and China due to factors like clean, renewable electricity costs, production methods, and available infrastructure. Based on data collected for this study, China produces green H₂ at 2.75 \$/kg, much lower than the 4–6 \$/kg in the U.S. [26], and expects to reduce electrolysis costs to 1 \$/kg by 2030 [27]. Despite the current costs associated with green H₂ production [28], a study confirms that grid-connected electrolysis in the Danish electricity market can produce H₂ at a cost of 3 €/kg (3.3 \$/kg) [29].

2.2.1. Example systems

Three different PtH systems are compared across Denmark, the U.S., and China. For each country, a representative example system is selected for the analysis.

In Denmark, the analysis draws inspiration from the concepts and ideas of GreenLab Skive with a PtH plant in Northern Jutland. Supported by the Danish Energy Authority and technology partners, GreenLab has constructed a 12 MW electrolysis plant to produce 10 million liters of green methanol annually from upgraded biogenic carbon dioxide [30]. With a direct 150 kV grid connection, 80 MW of onsite renewable electricity, and GreenLab's SymbiosisNet™ for optimized

energy/resource exchange, all H₂ produced will be 100% green. From this point forward, this system will be referred to as the Methanol Targeted (MT) system.

The U.S. example is a microgrid research station in California, operated by a Stanford University research group. The set-up currently includes PV and battery systems that meet the electricity demand of two modular building structures, with power capacities on the order of tens of kilowatts. A H₂ energy storage system has been proposed to serve as a backup supply, akin to a diesel generator, storing excess summer solar PV for higher winter demand. From now on, this system will be referred to as the Power Targeted (PT) system.

The information for the U.S. example is provided by the Atmosphere/Energy program at the Department of Civil and Environmental Engineering at Stanford University [31].

The PtH project in Zhangjiakou, Hebei, serves as a basis for the system in China. This area, abundant in wind and solar resources and designated as a National Renewable Energy Demonstration Zone, coordinates wind power and solar PV plants to transmit green electricity to nearby high-density cities [32]. Currently, China has seven H₂ storage facilities under construction or demonstration, with the Zhangjiakou project being the largest globally. It includes a 200 MW electrolyzer and 800 MWh of H₂ storage capacity [33].

Zhangjiakou's clean electricity was also used to support the Beijing 2022 Winter Olympics through more than 1000 fuel cell vehicles (FCVs) [34]. Following the Olympics, the FVC-oriented H₂ pathway started generating profit, providing a solution to the H₂ economy. Henceforth, this system will be referred to as the H₂ Fuel Targeted (HT) system.

2.2.2. System structure and operation

The systems' operation is modeled using a rule-based model, which makes decisions based on pre-defined rules. The model evaluates input data against these rules and applies the corresponding actions or conclusions by systematically checking each rule against the input conditions.

The model includes steps up to meeting the total H₂ or power demand, excluding further conversions to meet specific needs such as methanol or heating demands. The final steps are illustrated in Figs. 2–4 to highlight the differences in purpose and strategy at each location. These steps are indicated with dashed arrows.

Each system strives to meet the demand whenever possible. If there is no available power during a given hour, the demand will not be met. Conversely, if there is excess power and storage is full, the surplus power is curtailed.

All systems are stand-alone and not connected to any grid. The renewable capacity for the MT and HT systems consists of 70% wind and 30% solar, while the PT system's input is comprised entirely of solar power.

The methanol targeted system

The MT system is coupled with an alkaline electrolyzer (AEL) and H₂ storage. The renewable electricity generates green H₂ to meet direct H₂ demand as much as possible. Any surplus H₂ is stored as compressed gas in a tank for use when direct production falls short. H₂ is then used to produce steel, ammonia (primarily for fertilizer) or methanol or other synthetic fuels for long-distance transportation. Fig. 2 illustrates the energy flow within the system, with arrows indicating the direction of energy movement. Thicker arrows signify higher priority compared with thinner arrows. The system configuration is inspired by the previous work presented in [35].

The power targeted system

The PT system addresses an electricity demand rather than H₂ demand, using renewable electricity to meet this demand directly. Surplus electricity is stored in an electric battery, which can be discharged when solar power is insufficient. If excess electricity is generated when

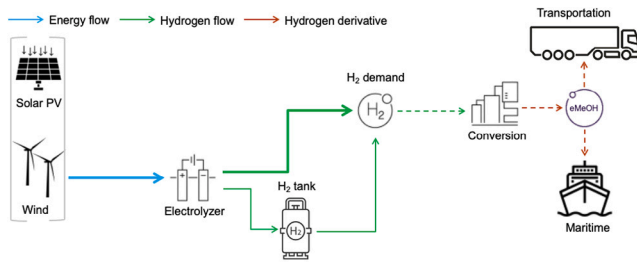


Fig. 2. Methanol Targeted system.

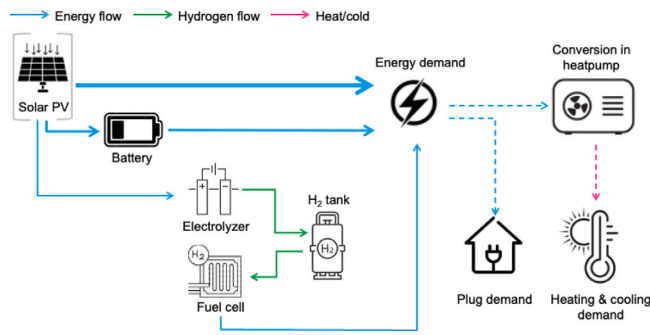


Fig. 3. Power Targeted system.

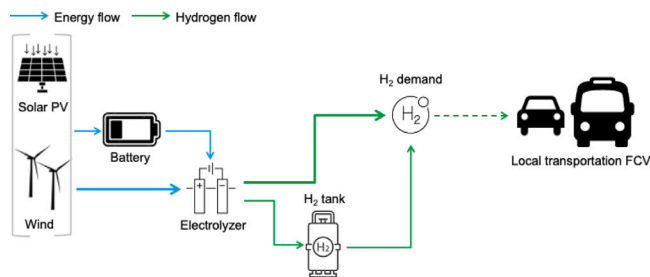


Fig. 4. Hydrogen Fuel Targeted system.

the battery is full, it is converted into H_2 and stored in a tank for long-term storage. In times of insufficient electricity production and a fully discharged battery, the stored H_2 can be converted back to electricity via a fuel cell. Gas leakage has not been considered for long-term H_2 storage. Fig. 3 illustrates the energy flow within the system.

The hydrogen fuel targeted system

The HT system is similar to the MT system but includes an additional battery for electricity storage as a secondary priority. The battery supports H_2 production when the supply is insufficient. The produced H_2 is directly used in FCVs for local transportation. Fig. 4 illustrates the energy flow within the system. The system configuration is inspired by the previous work presented in [36].

2.2.3. Data inputs

All systems utilize an hourly time series of wind and solar power as input to the rule-based model. Each location has geographically specific data, using coordinates from the three example systems: Skive in Denmark, California in the U.S., and Zhangjiakou in China. All inputs for the modeling can be seen in Table 1 to 3.

For Skive, wind and solar power data was provided by GreenLab [37], showing an average yearly capacity factor of 36% for wind and 13% for solar PV. The solar power data for California, with an average yearly capacity factor of 18%, was supplied by the research group at Stanford [31]. Wind power data for California, with an average yearly capacity factor of 13%, and renewable data for China, with

Table 1
Average yearly power capacity factors (%).

Location	Wind	Solar
Denmark	36 [37]	13 [37]
U.S.	13 [38]	18 [31]
China	13 [38]	20 [38]

Table 2
Technical specifications.

Electrolyzer	
Electrolyzer type	AEL
Power consumption rate at 100% load	4.33 kWh/Nm ³ [39]
Power consumption rate at 50% load	4.05 kWh/Nm ³ [39]
Power consumption rate at 25% load	3.84 kWh/Nm ³ [39]
H_2 density	0.089 kg/m ³ [40]
H_2 tank	
Round-trip efficiency	89% [40]
Charge and discharge ratio per hour	50% [31]
Initial storage level	80% [41]
Minimum storage level	5% [41]
Battery	
Round-trip efficiency	85% [42]
Power to energy ratio per hour	25% [31]
Initial storage level	50% [42]
Minimum storage level	4% [42]
Storage loss of stored energy	0.001% [31]
Fuel cell	
Round-trip efficiency	52% [43]
Gravimetric energy density	33.3 kWh/kg [40]
Converter	
Conversion efficiency	99% [39]

average yearly capacity factors of 13% for wind and 20% for solar PV, were all retrieved from Renewables.ninja [38]. Table 1 summarizes the capacity factors.

Each system features an hourly demand profile: H_2 demand for the MT and HT systems, and power demand for the PT system. The H_2 demand profile was provided by GreenLab [37], while the power demand profile was provided by the research team at Stanford [31]. The demand profiles reflect aggregated industrial off-grid consumers, with hourly demand exhibiting daily variations. These profiles are consistently maintained across all systems but are adjusted based on the installed capacity. A scaling factor is applied to the demand profile, determined by dividing the system's nameplate renewable capacity, c , by the nameplate renewable capacity of the reference system in the dataset, r_s , as follows: c/r_s . This factor is then multiplied by the demand profile.

Table 2 details the various technical specifications implemented in the systems. For an equal comparison, the parameters are kept uniform across all systems.

All systems include an AEL, whose efficiency varies. This entails that the electrolyzer has different power consumption rates at different operating levels, consistent with the principles for generating an H_2 production curve as described in [39].

To calculate the LCoE for comparing the different systems, both CAPEX and OPEX have been determined, incorporating location-specific adjustments where possible. Since the systems do not consume any fuel, this cost component is omitted from the LCoE calculation. Moreover, variable OPEX is assumed to be negligible due to its minimal contribution to overall system costs. Thus, the primary cost components considered are CAPEX and fixed OPEX, as summarized in Table 3. The cost estimates are representative of the year 2024 and do not account for future inflation.

The unit costs for Denmark and the U.S. are relatively similar, with some variations. However, China's costs are noticeably lower compared

Table 3
CAPEX and fixed annual OPEX cost components (all values are converted to USD (2024) using [17]).

Denmark	CAPEX [\$/kW]	Fixed annual OPEX [\$/kW-year]
Wind turbine	1249.8 [44]	18.2 [44]
PV	414.2 [44]	10.4 [44]
Electrolyzer	953.8 [45]	38.2 [45]
H ₂ tank	1733.5 \$/kg [40]	19.3 \$/kg-year [40]
Battery storage	721.0 [40]	0.6 [40]
Fuel cell	179.0 [43]	2.7 [46]
U.S.	CAPEX [\$/kW]	Fixed annual OPEX [\$/kW-year]
Wind turbine	1150.0 [47]	27.0 [47]
PV	700.0 [46]	7.0 [46]
Electrolyzer	720.0 [46]	2.1 [46]
H ₂ tank	1733.5 \$/kg [40]	19.3 \$/kg-year [40]
Battery storage	829.0 [47]	10.8 [47]
Fuel cell	179.0 [43]	2.7 [46]
China	CAPEX [\$/kW]	Fixed annual OPEX [\$/kW-year]
Wind turbine	320.0 [48]	3.2 [46]
PV	110.0 [49]	7.2 [46]
Electrolyzer	303.0 [50]	12.1 [45]
H ₂ tank	1733.5 \$/kg [40]	19.3 \$/kg-year [40]
Battery storage	126.0 [51]	4.3 [51]
Fuel cell	179.0 [43]	2.7 [46]
VoLL cost	10.0 \$/kWh [18]	

to the other systems, largely due to factors such as the cost of clean, renewable electricity, production methods, and existing infrastructure.

The discount rate, which is critical in determining the LCoE based on capital costs and future earnings, varies between projects and can impact LCoE results. In Denmark, the typical discount rate, based on historical data, is 4% [52]. However, it would currently be higher due to geopolitical factors. For the U.S., there is a wide range of reported rates, from 3% [53] to 8%–12% [54], with an 8% rate used for the LCoE evaluation. In China, four different forecasts for the 2025 discount rate [55] have been averaged, resulting in a rate of 6.82%.

A VoLL cost of 10 \$/kWh is applied for any unmet power demand for Denmark, the U.S., and China. This value is consistent with reported ranges, with estimates of VoLL between 4–40 \$/kWh for developed countries and 1–10 \$/kWh for developing countries, illustrating the broad variability depending on economic conditions and sectors [18]. For Europe, production function analyses show national VoLL values ranging from 3.2 €/kWh in Bulgaria to 15.8 €/kWh in the Netherlands, with Denmark specifically reported at 11.5 €/kWh [18]. Setting a uniform VoLL of 10 \$/kWh thus represents a balanced and reasonable estimate across the three countries analyzed, aligning with Denmark's reported value and fitting within the expected range for developed economies.

Given the varying lifespans of individual PtH system components (e.g., electrolyzers, storage units, power electronics), defining a unified system lifetime is challenging. For this study, a conservative system lifetime of 25 years is assumed, covering the operational period of most major components.

Replacement costs for components with shorter operational lives (such as batteries or specific electrolyzer stacks) are included within the fixed OPEX. This treatment ensures that the LCoE calculation realistically captures the total cost of ownership over the full system lifespan without introducing discontinuities or major reinvestment adjustments in the CAPEX. Fixed OPEX therefore includes not only routine operation and maintenance expenses but also the cost of necessary component replacements over the 25-year period. This approach provides a consistent cost basis across all systems and allows a fair comparison between different configurations.

Table 4

Optimized capacities for the electrolyzer, H₂ tank, battery storage, and fuel cell. Nameplate capacities have fixed wind turbine and solar PV capacities. The total renewable capacity is the same across scenarios for the different systems. In the MT and HT systems, wind accounts for 70% of the capacity and solar for 30%. In the PT system, solar makes up 100% of the renewable capacity.

Renewable capacity (MW)	Unit	100	300	500	2500	5000	10,000
MT system in Denmark							
Wind turbine	MW	70	210	350	1750	3500	7000
PV	MW	30	90	150	750	1500	3000
Electrolyzer	MW	20	61	101	505	1044	2087
H ₂ tank	ton	6	18	30	149	289	579
PT system in U.S.							
PV	MW	100	300	500	2500	5000	10,000
Electrolyzer	MW	8	26	45	265	537	1091
H ₂ tank	ton	2	5	8	42	85	170
Battery storage	MWh	74	220	361	1766	3517	6999
Fuel cell	MW	8	23	39	196	392	788
HT system in China							
Wind turbine	MW	70	210	350	1750	3500	7000
PV	MW	30	90	150	750	1500	3000
Electrolyzer	MW	31	100	172	929	1910	3987
H ₂ tank	ton	7	20	32	160	319	630
Battery storage	MWh	0	0	0	0	0	0

3. Results of the techno-economic evaluation

This section presents the analysis results for the three systems, comparing their operational strategies and economic performance. Section 3.1 illustrates each system's operation by showing their production profiles. Section 3.2 provides the LCoE results and offers an overview of the CAPEX structure.

3.1. Comparing system operation and sizing

The three systems are simulated across six different scenarios, each with a specific renewable capacity and various system sizes. These simulations are conducted to evaluate scaling effects and determine how different components are sized according to the renewable production capacity. Table 4 presents the scenarios for installed renewable capacity along with the optimized capacities for the electrolyzer, H₂ tank, battery storage, and fuel cell.

Comparing the MT and HT systems, where H₂ is the output, it is evident that the HT system requires a larger electrolyzer and H₂ tank to meet demand. This is primarily due to the differences in capacity factors for production, as shown in Table 1. The MT system benefits from a better capacity factor for wind compared with the HT system, which is the main reason for this discrepancy. While the capacity factor for PV is better in China, the advantage is smaller than the difference in wind's capacity factor among countries.

In the HT case, the optimization does not include battery capacity in the system. Despite the lower costs for battery storage compared with Danish and U.S. prices (see Table 3), the algorithm determines that prioritizing electrolyzer and H₂ storage capacity results in a better LCoE. The battery functions as a back-up electricity supply, but the H₂ storage is sufficient to store green H₂, making the battery storage unnecessary.

For the MT case, across all size scenarios, approximately 45% of renewable power is curtailed, and 50% of produced H₂ is not used, while only 2% of the demand is unmet.

In the HT case, the smallest system of 100 MW curtails 5% of renewable power, decreasing to 1% for the largest system of 10,000 MW. Unused H₂ ranges from 40% to 48% from the smallest to the largest system, and unmet H₂ demand remains around 5% for all scenarios.

In the PT case, power curtailment ranges from 47% to 41% from the smallest to the largest system, respectively. In these scenarios,

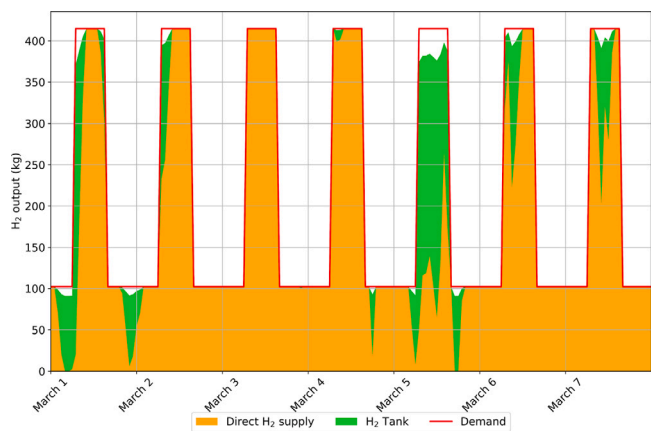


Fig. 5. MT system in Denmark: H₂ output first week of March.

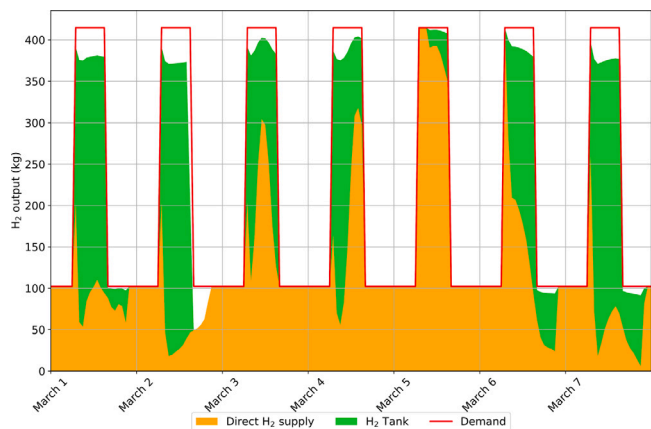


Fig. 6. HT system in China: H₂ output first week of March.

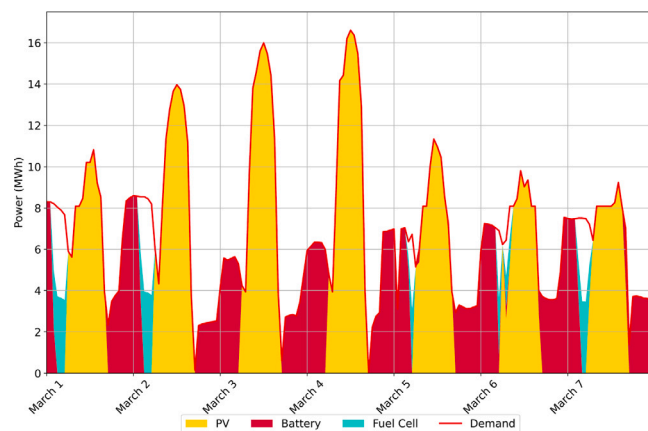


Fig. 7. PT system in the U.S.: power output first week of March.

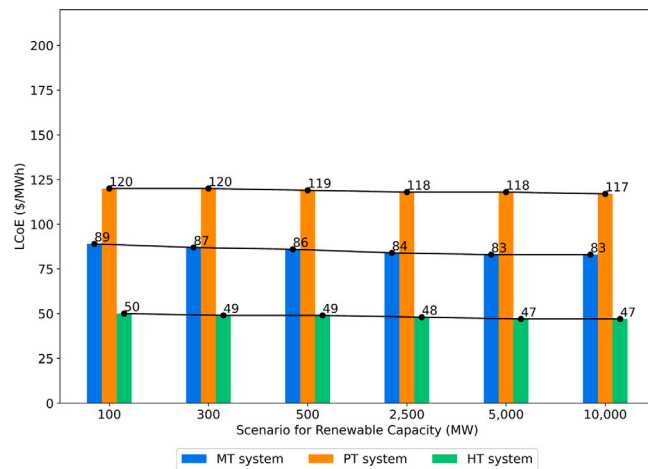


Fig. 8. LCoE of three different systems.

approximately 82% of the produced H₂ is not used for power balancing. Power demand remains unmet for 4%–5% of the total yearly demand.

To illustrate the operating patterns of the three different systems, the output for the first week of March is depicted in Figs. 5 to 7. March is selected as a representative month because it clearly demonstrates variations in the usage of different units within the systems. To ensure consistent and transparent system conditions, the H₂ storage tank was initialized at 80% of its total capacity. When renewable generation exceeds immediate demand, the tank is charged up to a maximum level of 100%. Conversely, during periods when generation is insufficient to meet demand, the stored H₂ is utilized, with the tank allowed to discharge down to a minimum operational level of 5%. This operational logic enables the system to flexibly balance variable renewable supply and H₂ demand over the course of the simulation week.

The MT (Fig. 5) and HT (Fig. 6) systems demonstrate how H₂ demand is primarily met directly by electrolysis, with additional support from H₂ storage at certain times. These differences arise due to variations in power production. In the PT system (Fig. 7), most power demand is covered by solar, with peaks during midday hours. At night, the battery system meets most of the demand. If the battery system becomes sufficiently depleted, the fuel cell activates, producing electricity from H₂. As observed, the H₂ fuel cell system is not used excessively (covering around 3% of the delivered power over a year) but still contributes to electricity generation and reduced outages. The fuel cell serves as a form of seasonal storage, primarily used at night during winter, while during summer, it operates for only a few hours.

3.2. Comparing costs

Fig. 8 illustrates the LCoE for the MT, PT, and HT systems across six different scenarios. An increase in system capacity does not lead to a large reduction in LCoE. Economies of scale only apply to the electrolyzer CAPEX, with all other costs remaining constant. The observed reduction in LCoE is due to the lower capacity cost for electrolyzers, which does not impact the total system construction costs. Only the PT system with 100 MW renewable capacity has an electrolyzer with a capacity below 20 MW, meaning the difference on electrolyzer CAPEX per capacity is small in all other cases.

As outlined in the introduction, the substantial cost differences between the HT system in China and other cases analyzed necessitate careful interpretation of the results, focusing on qualitative insights and relative trends rather than absolute cost values.

The MT system is more responsive to increased system size than the others, exhibiting a slightly larger decrease in LCoE. The HT system maintains the lowest LCoE due to generally lower costs, while the PT system's LCoE remains noticeably higher. It is important to focus on the relative differences in LCoE rather than the actual numbers, as the LCoE calculation only considers CAPEX, OPEX, refurbishment costs (factored into OPEX), and VoLL costs. This calculation excludes other factors such as decommissioning costs, abandonment costs, and taxes. The limitations of the LCoE calculation mean that the figures may not fully capture the complete financial picture of each system. While LCoE provides a useful metric for comparing the efficiency and cost-effectiveness of different energy systems, it does not account for

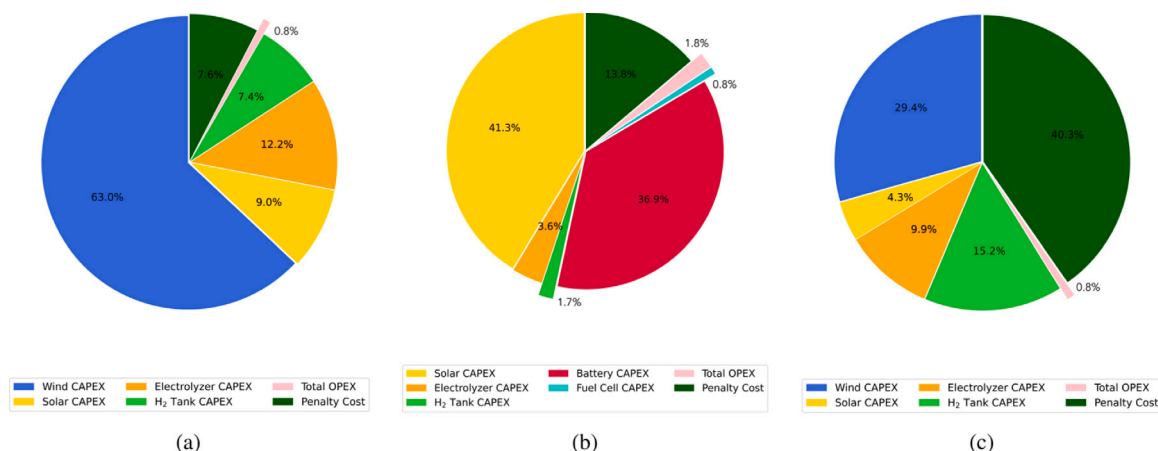


Fig. 9. Cost structure of 100 MW system including individual CAPEX, total OPEX and VoLL cost. Fig. 9(a) depicts the MT system, Fig. 9(b) the PT system and Fig. 9(c) the HT system.

country-specific cost, such as land lease or corporate tax, that could impact the total cost of ownership and operation. Therefore, despite the analytical value of LCoE comparisons, stakeholders should acknowledge the exclusions and incorporate additional financial metrics for a more complete assessment.

Parameters, such as land lease costs and corporate taxes, are not included in the LCoE calculation primarily because detailed, standardized data for these factors are often unavailable. Such costs are typically project-specific, confidential, and not transparently reported across different countries or companies. Including them would require heavy reliance on assumptions or rough estimates, introducing large uncertainties and reducing the reliability and comparability of the results. Furthermore, it is important to note that the standard definition of LCoE typically focuses on direct costs related to project investment, operation, and maintenance. It generally excludes external financial factors – such as land acquisition, taxation policies, or decommissioning costs – unless explicitly stated. To ensure methodological transparency and enable robust comparisons across the three cases, only universally accessible and verifiable cost components (CAPEX, OPEX, and refurbishment costs) are considered. Stakeholders are encouraged to complement the LCoE analysis with additional financial assessments when detailed, project-specific data are available.

In Fig. 9, the system cost structure is divided into percentage shares of the total cost for systems with 100 MW of renewable power. Comparing the MT (Fig. 9(a)) and HT (Fig. 9(c)) systems, which contain the same components and renewable power capacity, the MT system's CAPEX for wind power occupies a larger portion of the total costs. In contrast, the CAPEX for wind and solar power in HT holds roughly equal shares. In the MT system, the electrolyzer accounts for a larger share than the H₂ storage, while the opposite is true for the HT system. The HT system prioritizes investment in larger H₂ storage capacity, whereas the MT system relies more on direct delivery of H₂. OPEX makes up a minor share in both cases. As mentioned above, the MT system fails to meet 2% of demand, while the HT system falls short by 5%. This is reflected in the VoLL cost share: in the HT system, it is the largest, accounting for 40.3% of the total cost, amounting to \$30.7 million over the systems lifetime. The VoLL represents a large share of the total cost because the per unit VoLL cost is higher than that of the infrastructure. In the MT system, it ranks fourth, representing 7.6% of the total cost, equivalent to \$10.5 million.

The PT system's cost primarily comprises solar PV and battery CAPEX, which together account for 78.2%, seen in Fig. 9(b). Including the electrolyzer, H₂ storage, and fuel cell, its cost share is relatively small, totaling 6.1%. VoLL costs account for 13.8% due to an unmet demand of 4%.

An evaluation was also conducted to assess the system's cost structure excluding the H₂ components. In this scenario, PV CAPEX accounts

for 45.7% of the costs, the battery for 52.1%, OPEX for 0.5%, and the VoLL is reduced to 1.8% with an unmet demand of 3.6%. Additionally, 60.5% of the produced power is curtailed. By omitting H₂ components, the LCoE increases from \$120 to \$122, indicating that although VoLL costs decrease from a total of \$23 million to \$21 million, the battery CAPEX increases by nearly \$20 million due to the need for a larger battery size, leading to a higher LCoE.

Increasing the system's renewable capacity generally results in a slight increase in the shares of VoLL costs and renewable CAPEX, while the share of electrolyzer CAPEX decreases. In the PT system, the battery CAPEX share also decreases slightly.

3.2.1. Sensitivity of value of lost load cost

The VoLL cost for unmet demand is a sensitive parameter in the optimization problem, affecting system sizing, operation, and cost structure. The analysis was conducted with an initial VoLL cost of 10 \$/kWh to understand its impact on system performance. Adjusting this cost provide insights into how the systems are optimized and managed.

Generally, decreasing the VoLL cost leads to an increase in unmet demand, as operating with a lower delivery rate becomes more economical. Conversely, increasing the VoLL cost results in decreased unmet demand due to the higher expense associated with it.

The following VoLL costs have been tested for all systems: 0.3 \$/kWh, 3 \$/kWh, 10 \$/kWh, 15 \$/kWh, 30 \$/kWh and 60 \$/kWh.

In the MT system, adjusting the VoLL cost leads to less than a 0.5% change in unmet power demand. This suggests that the system's configuration is relatively stable across different VoLL costs, with most of the changes reflected in the share of VoLL costs itself. Curtailment rates remain largely unchanged. An increase in the VoLL cost results in a higher LCoE, without delivering substantial benefits in terms of system stability or demand fulfillment. The overall operation remains consistent, with the primary impact being an increase in the VoLL costs.

The HT system displays similar trends. While unmet demand is not notably affected, changes in VoLL costs have a more pronounced impact on the LCoE compared with the MT system. As VoLL costs increase, their share within the total system costs also rises, indicating the LCoE's high sensitivity to changes in VoLL.

For the PT system, the VoLL cost plays an important role in determining system configuration. A lower VoLL cost leads to high unmet demand, while an increase shifts the cost structure towards more expensive components, such as batteries, to minimize unmet demand. This shift results in higher LCoE as the system seeks to balance cost and performance.

The relatively small variation in LCoE values, despite large changes in renewable potential, reflects the systems' ability to redistribute

excess renewable energy via flexible infrastructure, such as H₂ production and storage, rather than directly reducing marginal energy costs. This systemic buffering effect limits the expected impact of renewable oversupply on LCoE. Additionally, the penalty cost in this study is applied as a static parameter. In practice, such costs would likely be dynamic and increase with renewable penetration levels, influencing both system optimization and overall costs. To capture this interaction more accurately, future work could explore the integration of variable penalty costs reflecting sector-specific renewable shares.

The sensitivity analysis illustrates the delicate balance between VoLL costs and system configuration. For the MT system, changes in VoLL costs do not affect unmet demand, indicating robust system design. However, in the HT and PT systems, VoLL costs have a more direct impact on LCoE, indicating a potential area for further optimization.

The PT system shows a clear relationship between VoLL costs and the reliance on expensive battery storage. This highlights the importance of VoLL cost calibration in influencing investment in renewable energy and storage solutions. Meanwhile, the HT system's sensitivity suggests that adjustments to VoLL costs could lead to more efficient system designs, potentially optimizing for both cost and performance.

Overall, this analysis underscores the need for careful consideration of VoLL costs in system planning and optimization, particularly as they relate to LCoE and demand fulfillment.

3.3. Crossing systems

In view of the cost differences, emphasis should be placed on system-level trends and integration patterns, where relative dynamics yield more meaningful insights than straightforward cost comparisons.

The three systems – MT, PT and HT – were evaluated separately because each one has a different configuration. It is important to understand how each system performs in various settings. To do this, each system configuration was tested in all three locations — Denmark, the U.S., and China. For example, the MT configuration (shown in Fig. 2) was also simulated using the power and economic data from the U.S. and China. This cross-location simulation was repeated for each of the three system configurations.

The large LCoE differences, particularly for the Chinese system, reflect broader structural factors outside the system scope. This section focuses on comparative trends in technology and integration to highlight systemic insights beyond absolute costs.

Fig. 10 illustrates how the LCoE varies when each system is implemented in the three different countries. Despite slight differences in the demand profiles, which are scaled for each location, the costs and renewable power production data remain consistent. This consistency means that the capacity optimization results in the same configuration for the MT and HT systems across all locations. Consequently, their LCoE is identical when compared across different countries. This consistency in system configuration underscores that the capacity factor of renewable energy sources is primarily determined by location-specific resource conditions. As a result, LCoE outcomes are predominantly influenced by location, while system design and operation can only optimize the use of the available resource(s) within given constraints. Among the three locations, China has the lowest LCoE for both the MT and HT systems (Fig. 10(c)), primarily due to lower investment costs compared to Denmark and the U.S., while the U.S. has the highest LCoEs.

The figures indicate that the PT system is the most expensive to operate in any location. This is because it is the most complex system, incorporating more components and a substantial portion of battery storage CAPEX. The PT system shows the most prominent change in LCoE between locations, with the lowest LCoE in China. In the U.S., the difference in LCoE between systems is much smaller than in other locations. In Denmark, the PT system's LCoE is 139% higher than that of the other systems. In China, the difference is 102%, while in the U.S., the PT system's LCoE is only 8% higher.

To better understand the cost differences, Fig. 11 displays the cost structures for the PT system in each location, using location-specific data. In Denmark, as shown in Figs. 10(a) and 11(a), the LCoE is the highest, largely due to VoLL costs. The system includes no H₂ capacity, as optimization determines that it is more economical to pay a VoLL for unmet demand, which is at 24%. The VoLL is substantial, amounting to \$138 million, with 58% of the produced power being curtailed. To improve power delivery and lower the LCoE, the VoLL should be increased to encourage the system to expand capacity. Adjustments are necessary for the PT system configuration in Denmark to achieve a lower LCoE, as the current unmet demand is too high.

In China, as shown in Figs. 10(c) and 11(c), the PT system achieves the lowest LCoE among the three countries. The cost structure reveals that the H₂ system contributes minimally to the total cost, while battery CAPEX takes up a large share. This indicates that the system prioritizes battery capacity to meet demand. The VoLL cost is low, with the system failing to meet demand only 3% of the time.

4. Discussion

This study compares three distinct Pth systems – MT, PT, and HT – located in Denmark, the U.S., and China, respectively. The research evaluates green H₂ systems across diverse geographical contexts, assessing their economic performance through simulation. The analysis covers LCoH and CAPEX structures to offer insights into the financial viability and investment potential of each system, while also examining the influence of cost factors on system operation and implementation.

The operational strategies of the three systems are tailored to align with their respective priorities in meeting demand. The Danish MT system and the Chinese HT system focus on the production of alternative fuels, while the U.S. PT system is designed to support secure power delivery, reflecting its role as a stabilizer in the grid. The operational analysis is confined to the primary product delivered by the H₂ system, without extending to the costs and energy flows associated with further conversions, such as power-to-heat or H₂-to-methanol. Future research could expand the model to optimize installed wind and solar capacities, thereby enhancing capacity factor utilization and aligning other unit capacities accordingly.

To ensure an unbiased comparison, key modeling parameters were held constant: renewable power capacities remained unchanged, all systems were demand-driven, and the objective was to minimize the LCoE. A uniform VoLL-based imbalance cost was imposed as a penalty for unmet demand. While this approach provides cross-case comparability, it also underscores the need for future research to explore how alternative penalty mechanisms may influence system performance. This work seeks to create a uniform basis for the comparative assessment of Pth system designs.

Location clearly influences costs: China demonstrates an overall cost advantage over Denmark and the U.S. However, this finding should be interpreted with caution, given the limitations in data availability and the representativeness of the selected studies. While the costs in Denmark and the U.S. are relatively similar, the analysis does not fully capture the potential variation in regional costs, particularly those driven by market conditions and policies.

The study also examines the effect of economies of scale, which appears marginal in systems with large capacities. The scaling effect was applied solely to electrolyzer CAPEX to isolate and assess its influence. Given that AEL technology has reached a high level of maturity, further cost reductions are primarily driven by scaling up production through supply-chain improvements [56]. A broader analysis could incorporate economies of scale across all system components, particularly at higher system capacities.

In comparison with the MT and HT systems, the PT system is more expensive, albeit with a moderately higher rate of demand satisfaction. The PT system is costly regardless of location, but may be viable in regions where the H₂ demand is relatively small. On the other hand,

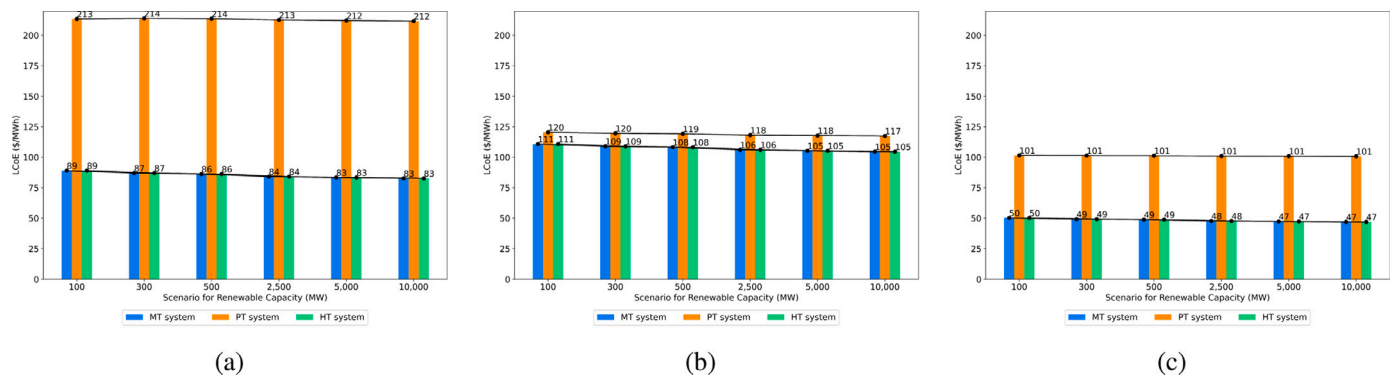


Fig. 10. LCoE for the three locations when analyzing the three systems. It is important to focus on the relative differences in LCoE rather than the actual numbers. Fig. 10(a) shows the LCoE for three different systems deployed in Denmark, utilizing Danish prices and renewable resources. Fig. 10(b) shows the LCoE for three different systems deployed in the U.S., utilizing U.S. prices and renewable resources. Fig. 10(c) shows the LCoE for three different systems deployed in China, utilizing Chinese prices and renewable resources.

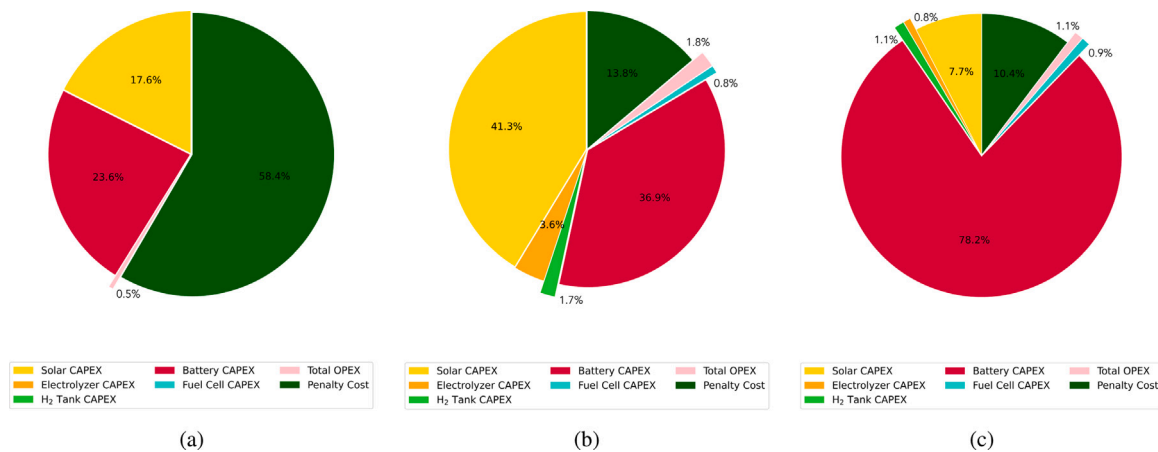


Fig. 11. The cost structure of a 100 MW PT system in different locations, where Fig. 11(a) shows the PT system in Denmark, Fig. 11(b) shows the PT system in the U.S., and Fig. 11(c) shows the PT system in China.

the MT and HT systems converge on the same configuration after cost optimization, suggesting that supplementing electrolyzer power input with battery storage is not cost-effective when H₂ output is prioritized. Conversely, when the main goal is power delivery – primarily supported by batteries – integrating an H₂ system can improve demand satisfaction, though at a higher cost and only in select locations.

This study underscores the complexity of designing and optimizing green H₂ systems across different geographical contexts. The findings suggest that, while cost optimization may yield similar configurations in systems with aligned objectives, achieving cost-effectiveness requires system designs that are closely adapted to local conditions. The results also emphasize the relevance of extending future research to include a broader range of economic and operational variables, including system-wide economies of scale and impacts of further energy conversions processes. The variation in LCoE across locations highlights a need for stakeholders to take into account regional infrastructure and cost dynamics in the planning and implementation of green H₂ projects.

This work positions itself within the existing H₂ value chain by concentrating on the upstream section of the H₂-to-X pathway, specifically through an emphasis on PtH. It primarily addresses the initial stages of H₂ generation and conversion. While the present scope is limited to upstream processes, the approach can be extended downstream to include applications in hard-to-abate sectors such as steel and chemical manufacturing. Flexibility in the solution design supports extension or coupling with other tools and technologies, enhancing relevance and utility across the H₂ ecosystem. To ensure optimal integration and effectiveness, it is essential to define clear boundary conditions that delineate the PtH project’s impact and interaction with existing systems.

By conducting a comparative analysis of PtH systems in Denmark, the U.S., and China, this study addresses a gap in the literature concerning the influence of regional factors on the systems’ LCoE. While previous studies have examined the cost-effectiveness of H₂ production under various scenarios, this research extends the analysis by concentrating on the regional differences in investment costs, renewable energy availability, and system optimization strategies, and integrating them into a unified scheme. The findings emphasize the need for regional assessments when deploying H₂-based energy systems, demonstrating that regional differences can influence the economic viability and design of PtH systems. These insights provide guidance for scaling PtH systems strategically and supporting the global transition to carbon-neutral energy solutions.

5. Conclusion

This study presents an evaluation and comparison of PtH systems in Denmark, China, and the U.S. The analysis reveals distinct cost trends within each region, with China demonstrating lower overall CAPEX and OPEX for system components. Additionally, regional weather patterns have a considerable effect on the capacity factors of renewable electricity sources.

The three systems examined – MT, PT, and HT – vary in design and operational strategy. Their cost-effectiveness is assessed by minimizing the LCoE through the Hooke–Jeeves algorithm. For large-scale setups, the impact of electrolyzer CAPEX scaling on LCoE remains modest.

The limited sensitivity of LCoE to changes in renewable potential is attributed to the system’s capacity to redistribute excess renewable

energy via flexible infrastructure, while the model's use of a static penalty cost may underestimate cost variations associated with higher renewable penetration.

Optimization drives the MT and HT systems to adopt identical components, which leads to their operation under similar conditions. However, their cost structures differ. The MT system proves more robust against variations in VoLL costs, while the HT system displays greater volatility in both cost structure and demand satisfaction rates.

Compared with the PT system, the MT and HT systems yield lower LCoEs. The PT system consistently incurs the highest costs across all locations and exhibits substantial cost variation by region. The PT system in the U.S. exhibits the highest use of H₂ with a fuel cell backup for grid electricity.

The comparative analysis indicates that the economic viability of PtH systems is largely determined by system design choices, operational strategies, and associated costs. The findings emphasize the importance of tailoring PtH system designs to local conditions to achieve optimal cost-effectiveness.

Finally, while the analysis highlights key trends in system configurations and integration strategies, the substantial cost differences – notably in the Chinese case – emphasize the need to interpret the results within regional cost frameworks and broader system contexts, rather than relying on absolute cost values alone.

This work advances the field by offering evidence-based insights into how regionally optimized PtH system configurations can enable more strategic and cost-effective scaling of green H₂. These insights are relevant for both scientific research and practical energy transition planning worldwide.

CRediT authorship contribution statement

Elisabeth Andreae: Writing – original draft, Visualization, Validation, Software, Resources, Methodology, Investigation, Formal analysis, Data curation, Conceptualization. **Yuanbei F. Fan:** Writing – review & editing, Software, Methodology. **Marianne Petersen:** Writing – review & editing, Conceptualization. **Shi You:** Writing – review & editing, Supervision. **Henrik W. Bindner:** Writing – review & editing, Supervision. **Mark Z. Jacobson:** Writing – review & editing, Supervision.

Declaration of Generative AI and AI-assisted technologies in the writing process

During the preparation of this work, the main author for writing the original draft used ChatGPT for refining the language. After using this tool/service, the main author reviewed and edited the content as needed and takes full responsibility for the content of the publication.

Declaration of competing interest

The authors declare that they have no known competing financial interests or personal relationships that could have appeared to influence the work reported in this paper.

Acknowledgments

The authors wish to express their gratitude to Daniel J. Sambor from Stanford University for his valuable contributions in providing the essential background needed to understand the operation of the microgrid site managed by the research group at Stanford.

Data availability

Data will be made available on request.

References

- [1] Danish Energy Agency. Power-to-x. 2022, URL <https://ens.dk/ansvarsomraader/power-x-og-groen-brint>.
- [2] Baral S, Šebo J. Techno-economic assessment of green hydrogen production integrated with hybrid and organic rankine cycle (ORC) systems. *Heliyon* 2024;10(4). <http://dx.doi.org/10.1016/j.heliyon.2024.e25742>.
- [3] Wolf N, Tanneberger MA, Höck M. Levelized cost of hydrogen production in northern africa and europe in 2050: A Monte Carlo simulation for Germany, Norway, Spain, Algeria, Morocco, and Egypt. *Int J Hydrog Energy* 2024;69:184–94. <http://dx.doi.org/10.1016/j.ijhydene.2024.04.319>.
- [4] Urs RR, Chadly A, Al Sumaiti A, Mayyas A. Techno-economic analysis of green hydrogen as an energy-storage medium for commercial buildings. *Clean Energy* 2023;7(1):84–98. <http://dx.doi.org/10.1093/ce/zkac083>.
- [5] Luo Z, Hu Y, Xu H, Gao D, Li W. Cost-economic analysis of hydrogen for China's fuel cell transportation field. *Energies* 2020;13(24). <http://dx.doi.org/10.3390/en13246522>.
- [6] Superchi F, Mati A, Carcasci C, Bianchini A. Techno-economic analysis of wind-powered green hydrogen production to facilitate the decarbonization of hard-to-abate sectors: A case study on steelmaking. *Appl Energy* 2023;342. <http://dx.doi.org/10.1016/j.apenergy.2023.121198>.
- [7] Zheng Y, Huang C, You S, Zong Y. Economic evaluation of a power-to-hydrogen system providing frequency regulation reserves: a case study of Denmark. *Int J Hydrog Energy* 2023;48(67):26046–57. <http://dx.doi.org/10.1016/j.ijhydene.2023.03.253>.
- [8] Zheng Y, You S, Huang C, Jin X. Model-based economic analysis of off-grid wind/hydrogen systems. *Renew Sustain Energy Rev* 2023;187. <http://dx.doi.org/10.1016/j.rser.2023.113763>.
- [9] Makepeace RW, Tabandeh A, Hossain MJ, Asaduz-Zaman M. Techno-economic analysis of green hydrogen export. *Int J Hydrog Energy* 2024;56:1183–92. <http://dx.doi.org/10.1016/j.ijhydene.2023.12.212>.
- [10] Jacobson MZ, von Krauland AK, Song K, Krull AN. Impacts of green hydrogen for steel, ammonia, and long-distance transport on the cost of meeting electricity, heat, cold, and hydrogen demand in 145 countries running on 100% wind-water-solar. In: *Smart energy*. 11, Elsevier Ltd; 2023, <http://dx.doi.org/10.1016/j.segy.2023.100106>.
- [11] Jacobson MZ. Batteries or hydrogen or both for grid electricity storage upon full electrification of 145 countries with wind-water-solar? *IScience* 2024;27(2). <http://dx.doi.org/10.1016/j.isci.2024.108988>.
- [12] Curcio E. Techno-economic analysis of hydrogen production: Costs, policies, and scalability in the transition to net-zero. *Tech. rep.*
- [13] Loh YY, Ng DK, Andiappan V. Techno-economic optimisation of green and clean hydrogen production. *Process Integr Optim Sustain* 2024. <http://dx.doi.org/10.1007/s41660-024-00439-x>.
- [14] María Villarreal Vives A, Wang R, Roy S, Smallbone A. Techno-economic analysis of large-scale green hydrogen production and storage. *Appl Energy* 2023;346. <http://dx.doi.org/10.1016/j.apenergy.2023.121333>.
- [15] Kochenderfer MJ, Wheeler TA. *Algorithms for Optimization*. The MIT Press; 2019, URL <http://mitpress.mit.edu>.
- [16] Badouard T, Moreira De Oliveira D, Yearwood J, Torres P. Final report cost of energy (LCOE): Study on energy costs, taxes and the impact of government interventions on investments in the energy sector. *Tech. rep, Enerdata, Trinomics; 2020*.
- [17] Xe Currency Converter, URL <https://www.xe.com/currencyconverter/convert/?Amount=1&From=EUR&To=USD>.
- [18] A. L. S. G, T. B, T. E. Societal appreciation of energy security volume 1: Value of lost load-households (EE, NL and PT). 2018, <http://dx.doi.org/10.2760/139585>, URL <https://ec.europa.eu/jrc>.
- [19] Lazard. *Lazard's Levelized Cost of Hydrogen Analysis*. *Tech. rep., 2021*.
- [20] Danish Ministry of Climate. Regeringens strategi for Power-to-X. *Tech. rep., 2021*, URL https://ens.dk/sites/ens.dk/files/ptx/strategy_ptx.pdf.
- [21] Reglobal. Green hydrogen production and utilisation in Denmark. 2023, URL <https://reglobal.org/green-hydrogen-production-and-utilisation-in-denmark/>.
- [22] Green Hydrogen Organisation. Denmark green hydrogen vision, URL <https://gh2.org/countries/denmark>.
- [23] USDepartment of Energy. *U.S. National Clean Hydrogen Strategy and Roadmap*. *Tech. rep., 2023*.
- [24] Fujimura K, Toyama N. China goes big on green hydrogen using renewable energy surplus. *NikkeiAsia* 2024. URL <https://asia.nikkei.com/Business/Energy/China-goes-big-on-green-hydrogen-using-renewable-energy-surplus>.
- [25] CGTN. China tops world in hydrogen stations, fueling a clean energy future. 2024, URL <https://news.cgtn.com/news/2024-01-01/China-tops-world-in-hydrogen-stations-fueling-a-clean-energy-future-1q0r4UCQF0s/p.html>.
- [26] Hinote J. Two sides of the same coin: U.S.-China green hydrogen strategies. *China USA Focus* 2023. URL <https://www.chinausfocus.com/energy-environment/two-sides-of-the-same-coin-us-china-green-hydrogen-strategies>.
- [27] Ouyang A. Can China make hydrogen electrolyzers cheap as it did for solar? *Marco Polo* 2023. URL <https://macropolo.org/china-hydrogen-electrolyzers-cheap-solar/?rp=m>.

- [28] IRENA. Green hydrogen cost reduction. Tech. rep., 2020, URL www.irena.org/publications.
- [29] Ghaebi Panah P, Cui X, Bornapour M, Hooshmand RA, Guerrero JM. Marketability analysis of green hydrogen production in Denmark: Scale-up effects on grid-connected electrolysis. *Int J Hydrog Energy* 2022;47(25):12443–55. <http://dx.doi.org/10.1016/j.ijhydene.2022.01.254>.
- [30] Christopher Sorensen. Project one-pager GreenLab Skive.
- [31] Stanford university, department of civil and environmental engineering, atmosphere and energy programme. 2024.
- [32] Zhang G, Zhang J, Xie T. A solution to renewable hydrogen economy for fuel cell buses – A case study for Zhangjiakou in north China. *Int J Hydrog Energy* 2020;45(29):14603–13. <http://dx.doi.org/10.1016/j.ijhydene.2020.03.206>.
- [33] Liu T, Yang Z, Duan Y, Hu S. Techno-economic assessment of hydrogen integrated into electrical/thermal energy storage in PV+ wind system devoting to high reliability. *Energy Convers Manage* 2022;268. <http://dx.doi.org/10.1016/j.enconman.2022.116067>.
- [34] The State Council of The People's Republic of China. Clean energy vehicles take road to future at the winter olympics. 2022, URL https://english.www.gov.cn/news/topnews/202202/09/content_WS6203209ac6d09c94e48a4dc8.html.
- [35] Zheng Y, You S, Bindner HW, Münster M. Optimal day-ahead dispatch of an alkaline electrolyser system concerning thermal–electric properties and state-transitional dynamics. *Appl Energy* 2022;307. <http://dx.doi.org/10.1016/j.apenergy.2021.118091>.
- [36] Zhang X, Pei W, Mei C, Deng W, Tan J, Zhang Q. Transform from gasoline stations to electric-hydrogen hybrid refueling stations: An islanding DC microgrid with electric-hydrogen hybrid energy storage system and its control strategy. *Int J Electr Power Energy Syst* 2022;136. <http://dx.doi.org/10.1016/j.ijepes.2021.107684>.
- [37] GreenLab skive . 2022.
- [38] Renewables.ninja. 2024, URL <https://www.renewables.ninja>.
- [39] Andreae E, You S, Bindner HW, Petersen M. An assessment of electrolyser portfolio for offshore hydrogen production considering its key properties - efficiency, ramp rate and capacity. *Journal of physics: conference series* 2023;2626(1). <http://dx.doi.org/10.1088/1742-6596/2626/1/012013>.
- [40] Danish Energy Agency (DEA). Technology Data for Energy storage. Tech. rep., 2023, URL <http://www.ens.dk/teknologikatalog>.
- [41] Zheng Y, You S, Bindner HW, Münster M. Optimal day-ahead dispatch of an alkaline electrolyser system concerning thermal–electric properties and state-transitional dynamics. *Appl Energy* 2022;307. <http://dx.doi.org/10.1016/j.apenergy.2021.118091>.
- [42] Andreae E. Sizing hybrid power plants under round-the-clock tender compliance in India. 2019, URL www.elektro.dtu.dk.
- [43] Kleen G, Gibbons W, Fornaciari J. DOE hydrogen program record 23002: Heavy-duty fuel cell system cost – 2022. Tech. rep., Department of Energy, United States of America; 2023, URL https://www.hydrogen.energy.gov/pdfs/review22/fc339_weber_borup_2022_o.pdf.
- [44] Danish Energy Agency (DEA). Technology data for energy plants for electricity and district heating generation. Tech. rep., 2023, URL <http://www.ens.dk/teknologikatalog>.
- [45] Danish Energy Agency (DEA). Technology data for renewable fuels. Tech. rep., 2024, URL <http://www.ens.dk/teknologikatalog>.
- [46] Lazard. LCOE+. Tech. rep., 2023.
- [47] NREL. Annual technology baseline, 2023 electricity ATB technologies and data overview. 2023.
- [48] International Renewable Energy Agency (IRENA). Zhangjiakou energy transformation strategy 2050: Pathway to a low-carbon future. Tech. rep., 2019, URL www.irena.org.
- [49] China solar panel costs plunge in 2023, 60% cheaper than US. *Asia Financ* 2023. URL <https://www.asiafinancial.com/china-solar-panel-costs-plunge-in-2023-60-cheaper-than-us>.
- [50] Lichner C. Electrolyzer prices – what to expect. *Pv Mag* 2024. URL <https://www.pv-magazine.com/2024/03/21/electrolyzer-prices-what-to-expect/?fbclid=IwAR2J9JYOBKk1ibK7Go4vFg8-EVluMDGM-dv3s78JyKEZ0qpW6EZKnnqAdk>.
- [51] Catsaras O. Lithium-ion battery pack prices hit record low of \$139/kwh. *BloombergNEF* 2023. URL <https://about.bnef.com/blog/lithium-ion-battery-pack-prices-hit-record-low-of-139-kwh/>.
- [52] Danish Energy Agency (DEA). Finding your cheapest way to a low carbon future the danish leveled cost of energy calculator. Tech. rep.
- [53] Kneifel JD, Lavappa P. Energy price indices and discount factors for life-cycle cost analysis– 2023: annual supplement to NIST handbook 135. 2023.
- [54] Tenney J. California community electricity providers issue \$5 billion in bonds for clean energy projects. *Ava Community Energy* 2023. URL <https://avaenergy.org/news-and-events/california-community-electricity-providers-issue-5-billion-in-bonds-for-clean-energy-projects/>.
- [55] Rong Y, Sun X. Discount rate of China's new energy power industry. *Energy Eng: J Assoc Energy Eng* 2022;119(1):315–29. <http://dx.doi.org/10.32604/EE.2022.015485>.
- [56] Reksten AH, Thomassen MS, Møller-Holst S, Sundseth K. Projecting the future cost of PEM and alkaline water electrolyzers; a CAPEX model including electrolyser plant size and technology development. *Int J Hydrog Energy* 2022;47(90):38106–13. <http://dx.doi.org/10.1016/j.ijhydene.2022.08.306>.